HHS Public Access

Author manuscript

Nat Mater. Author manuscript; available in PMC 2016 July 09.

Published in final edited form as:

Nat Mater. 2016 April ; 15(4): 407–412. doi:10.1038/nmat4539.

Underwater contact adhesion and microarchitecture in polyelectrolyte complexes actuated by solvent exchange

Qiang Zhao[#1], **Dong Woog Lee**[#2], **B. Kollbe Ahn**[#3], **Sungbaek Seo**[3], **Yair Kaufman**[2], **Jacob N. Israelachvili**[1,2,*], and **J. Herbert Waite**[4,*]

[1]Materials Research Laboratory, University of California, Santa Barbara, California 93106, USA.

[2]Chemical Engineering, University of California, Santa Barbara, California 93106, USA.

[3]Marine Science Institute, University of California, Santa Barbara, California 93106, USA.

[4]Molecular, Cellular and Developmental Biology, University of California, Santa Barbara, California 93106, USA.

[#] These authors contributed equally to this work.

Abstract

Polyelectrolyte complexation is critical to the formation and properties of many biological and polymeric materials, and is typically initiated by aqueous mixing[1] followed by fluid–fluid phase separation, such as coacervation[2–5]. Yet little to nothing is known about how coacervates evolve into intricate solid microarchitectures. Inspired by the chemical features of the cement proteins of the sandcastle worm, here we report a versatile and strong wet-contact microporous adhesive resulting from polyelectrolyte complexation triggered by solvent exchange. After premixing a catechol-functionalized weak polyanion with a polycation in dimethyl sulphoxide (DMSO), the solution was applied underwater to various substrates whereupon electrostatic complexation, phase inversion, and rapid setting were simultaneously actuated by water–DMSO solvent exchange. Spatial and temporal coordination of complexation, inversion and setting fostered rapid (~25 s) and robust underwater contact adhesion ($W_{ad} \geq 2$ J m^{-2}) of complexed catecholic polyelectrolytes to all tested surfaces including plastics, glasses, metals and biological materials.

The wet adhesion of mussels and sandcastle worms involves an exquisite blend of catechol chemistry, polyelectrolyte complexes and supramolecular architecture[6,7]. Catechol chemistry[8,9] and polyelectrolyte complexes[7,9] have been imaginatively translated into

[*] jacob@engineering.ucsb.edu; herbert.waite@lifesci.ucsb.edu.

Author contributions

Q.Z. and J.H.W. conceived the concept of materials processing. Q.Z. was responsible for the experimental part with input from B.K.A. who advised on PAAcat synthesis, SFA, confocal microscopy and FTIR. S.S. synthesized PAAcat copolymers. D.W.L. planned and performed SFA experiments and analysed the data. D.W.L. and B.K.A. performed and analysed confocal microscope experiments. Q.Z., D.W.L., B.K.A. and J.H.W. analysed data and wrote the paper. All authors read and commented on the paper. J.H.W. supervised the overall project.

Additional information

Supplementary information is available in the online version of the paper.

Competing financial interests

The authors declare no competing financial interests.

synthetic adhesives[10,11]; however, the supramolecular architecture, particularly the micro- and nanoporosity, of mussel and worm holdfasts[12–14] remains largely unexplored. A recent report that the adhesive fracture energy of individual mussel plaques is >1,000 times greater than the adhesion energy of the stickiest protein[15] suggests that effective translation of mussel and sandcastle worm adhesion would benefit from an integrative strategy combining catechols, polyelectrolytes and architectures, for example, into a single platform, but is this technically possible?

Early studies by Bungenberg de Jong[16] demonstrated that structured fluids could be prepared from aqueous polyelectrolyte mixtures known as complex coacervates, which, with their combined properties of high density, high diffusivity and low interfacial tension[17], seem well suited for adhesion[18]. Ternary mixtures of gelatin–gum Arabic–nuclein, for example, self-organize into dense droplets that are further sub-compartmentalized into cells. Although such mixing strategies are easy to implement, droplet coalescence is slow and prone to much variation with respect to polymers and solution conditions. Triggered bulk setting of coacervates is unavailable and polymeric adhesives that are fully implemented underwater (without pre-immersive dry curing or applied compressing pressure) remain challenging[19]. Thus, new strategies to develop polyelectrolyte complexation beyond waterborne mixing are needed.

Compared with water, most organic solvents possess lower dielectric constants (ε) and thereby tend to suppress ionization in weak polyelectrolytes[20]. This feature offers opportunities in that certain weak polyelectrolytes can be tuned between neutral and charged by changing the medium from an organic (low ε) to water (high ε)-based solvent. Building on this, we have explored the ‘solvent exchange’ concept for engineering complexation and microarchitecture in polyelectrolytes. To this end, organic solubility of constituent water-soluble polyelectrolytes was enhanced by pairing the cationic polyelectrolyte with an amphipathic bulk anion[21]. From here, the solvent exchange concept readily lends itself to a range of materials chemistries. By translating key chemical features of sandcastle worm cement proteins into starting polyelectrolytes, the new method renders rapid and robust wet adhesion on a broad range of solid substrates, in stark contrast to synthetic adhesives that are normally undermined by moisture[22].

The sandcastle worm builds concrete structures underwater by selecting particles of suitable dimensions and composition from its surroundings and gluing these together with a protein mortar from its ‘building organ’ (Fig. 1a). The mortar has been compared to a complex coacervate—a phase-separated fluid composed of oppositely charged polypeptides: polyanionic peptides rich in *O*-phosphoserine and cationic peptides with high lysine and arginine[9]. On deposition onto particle surfaces, the coacervate undergoes a three-stage maturation into a porous solid that is characterized by a phase inversion of coacervate fluid, insolubilization of protein metal ion complexes, followed by a slower covalent cure based on crosslinks formed by oxidized 3,4-dihydroxy-L-phenylalanine (L-DOPA), finally assuming the shape of the tubular walls[18]. We designed two polyelectrolytes satisfying both ‘solvent exchange’ requirements and wet chemistry of sandcastle worm mortar (Fig. 1b). The first is a poly(acrylic acid) functionalized with catechols (30 mol%, PAAcat, Supplementary Figs 1–4), and the second a quaternized chitosan that is ion-paired with bis(trifluoromethane-

sulphonyl)imide (Tf_2N^-) (QCS-Tf_2N, Supplementary Fig. 5). Unlike unmodified chitosan, QCS-Tf_2N is soluble in dimethyl sulphoxide (DMSO) owing to favourable interactions between bulk Tf_2N and DMSO (ref. 21).

QCS-Tf_2N and PAAcat were dissolved in DMSO together with a dye for visibility, and the mixture was extruded from a syringe onto an underwater glass slide over which it readily spread (see Methods). Cartoons sketched onto underwater surfaces (Fig. 1b and Supplementary Movie 1) set after as little as 25 s, and achieved sufficient adhesion to glass surfaces to withstand water blasting (2 bar, 15 s); the adhesive set for longer time (1 h) in water resisted a stronger water jet (30 bar, Supplementary Fig. 6). The adhesive withstood 1 h in boiling water and reimmersion in DMSO (Supplementary Fig. 7) with remarkably versatile adhesion to solid surfaces including polymers, metals and glasses (Supplementary Fig. 8), as well as natural surfaces, for example, mussel shell, stone, leaf and wood (Fig. 1c and Supplementary Fig. 9). The casting of QCS-Tf_2N/PAAcat solutions with embedded cotton tethers onto submerged glass slides withstood a 20 g load (Fig. 1d). The solvent exchange process also enables the bonding of two glass slides in water without applied compressive forces (Supplementary Fig. 10). These properties suggest that blended polyelectrolyte solutions have potential as underwater glues, coatings or paints.

The wet adhesion mechanism was investigated using glass slides as test surfaces. Owing to the lower dielectric constant of DMSO (ε =47.2, T =20°C), most acrylic acid groups (COOH) on PAAcat remain unionized in DMSO (Fig. 2a, t_s =0 min). Thus, PAAcat and QCS-Tf_2N coexist uncomplexed in DMSO (Supplementary Fig. 11). Given DMSO's miscibility in water, solvent exchange took place when the polymer blend solution was extruded into water (Fig. 2a, $t_s > 0$ min). By diffusing into the polymer solution, water induced deprotonation of PAAcat, converting it from a neutral state into a negatively charged one (Fig. 2a, top scheme). The deprotonation step initiated electrostatic attraction between negative PAAcat and positive QCS-Tf_2N, and formation of a fluidic complex coacervate intermediate phase (Supplementary Fig. 12 and Supplementary Movie 2). Characteristic Tf_2N anion peaks (1,050 cm^{-1}, 1,190 cm^{-1}) of the adhesive (t_s = 60 min) disappeared (Fig. 2b), which agrees with the EDS result that negligible Tf_2N remained in the same adhesive (Supplementary Table 1). Given that counter-ion release is quantitatively associated with complexation[2], both analyses indicate that electrostatic complexation between QCS and PAAcat occurs during the water–DMSO solvent exchange.

Solvent exchange processing offers advantages well suited to wet adhesion. First, precise spatial positioning of deposition was demarcated by spontaneous setting along the top surface of the polymer solution that progressed normally into the solution owing to the top-down diffusion of water (Supplementary Fig. 13). The solid peripheral boundary effectively confined the underlying polymers preventing dispersion during solvent exchange. This top-down processing also allowed for time-dependent interfacial interactions such as catechol chemisorption, electrostatic/hydrophobic forces, and/or hydrogen bonding depending on surfaces types (Supplementary Fig. 14). For glass surfaces, hydrogen bonding between glass (silanol groups) and hydroxyl groups from PAAcat and QCS is likely to dominate interfacial interactions. Surface forces apparatus (SFA) measurements show that adsorption thicknesses of the QCS-Tf_2N and PAAcat applied separately (t_s =1 h) to glass after water blasting were

~3 and ~40 nm, respectively. This suggests that PAAcat has a stronger interaction with glass, further supported by the poor adhesion of QCS/PAA without catechol (Supplementary Fig. 15). The importance of catechol groups for wet adhesion was further verified by the poor wet adhesion when catechol groups were made unavailable for interfacial interaction by chelation with Fe^{3+} ions (Supplementary Fig. 16). Moreover, solvent exchange complexation facilitated efficient and spontaneous setting, which has been challenging to engineer into many synthetic complex coacervates[11]. An immediate set based on electrostatic complexation produced rapid wet adhesion, whereas oxidative crosslinking between catechol groups required ~24 h without periodate (Supplementary Fig. 17). In control experiments, coatings deposited from only QCS-Tf_2N or PAAcat solutions showed negligible wet adhesion (Supplementary Fig. 15). This confirms the importance of network complexation between QCS-Tf_2N and PAAcat for cohesion.

The solvent exchange offers new strategies for engineering higher order coating architectures, such as porous solids (Fig. 2 and Supplementary Fig. 18) reminiscent of the sandcastle worm cement (Fig. 1a) and mussel plaques[6]. Porosity correlates with catechol density in PAAcat, that is, the wet adhesive became incrementally more trabecular with increasing catechol functionalization of PAA (Supplementary Figs 19 and 20), but greater porosity also significantly improved wet adhesion (Supplementary Fig. 21). The latter trend is not unexpected given previous investigations of increased fracture energy in biological cellular structures (for example, cork, bones, coral)[23,24]. Although much is known about fabricating porous solids from phase separation and emulsion inversion of polymers[25], these are not endowed with wet adhesion and have not been duplicated using polyelectrolytes.

The effect of water-mediated setting was investigated by fluorescence microscopy and SFA (Supplementary Methods). The fluorescence intensity of an added reporter dye ‘DIL’ (1,1′-dioctadecyl-3,3,3′3′-tetramethyl indocarbocyanineperchlorate; DMSO-soluble and water-insoluble) increased with increasing setting time (Fig. 3a), and plateaued after ~5 min. This is due to the increasing concentration of dye molecules in the pathlength (1.626 μm) because the volume of the enclosed polymer solution underwent >90% shrinkage during solvent exchange (Supplementary Fig. 22). Furthermore, water–DMSO solvent exchange kinetics correlate with the adhesion strength of the polymer to glass (Fig. 3b). After a critical setting time (t_s ~ 1.5 min), the adhesion force increased sharply up to F_{ad} ~ 200 mN at t_s = 10 min, eventually reaching an asymptote of equivalent adhesion energy of W_{ad} ~ 2 J m^{-2}, using Johnson–Kendal–Roberts theory ($W_{ad} = F_{ad}/1.5\pi R$; ref. 26), where R is the radius of curvature of the lower spherical disc. Control experiments showed that QCS-Tf_2N, PAAcat, PAA and QCS-Tf_2N+PAA solutions exhibited little to no adhesion even after t_s > 1 h in water, suggesting a synergy between electrostatic complexation and catechol chemistry with consequences for the wet adhesion (Supplementary Fig. 23). Water blasting experiments (Fig. 3c) support the SFA results; that is, longer setting times (t_s = 10 min) withstood stronger blasting. Curiously, the coating, once set, was erasable by abrasion with nitrile rubber (worn as a glove) under comparable pressures (Supplementary Fig. 24). The fully set coating surface is highly hydrated, making it difficult to remove by hydrophilic shearing (water blasting) owing to ‘hydration lubrication’ generated by the fluidity of hydration layers on the polymer surface[27,28]. However, a nitrile rubber surface is relatively

hydrophobic (or less hydrophilic) and can remove the hydrated water layer on polymer coatings by imposing a higher friction force, f, at the polymer–rubber interface.

To confirm and quantify our hypothesis that hydration layers enhance adhesion by reducing friction, we performed underwater friction experiments in SFA (Fig. 4), where we sheared the coating against a highly hydrophilic substrate (mica). Three distinct (load-dependent) lubrication regimes were observed as characterized by differences in the friction coefficients, $\mu = \partial f / \partial L$. When the load, L, was smaller than ~17 mN (regime I), polymer coatings remained intact, undamaged by shear, and dominated by hydration lubrication, which gave a low $\mu = 0.16$. When the load exceeded ~17 mN, the polymer coating started to peel off, leaving behind polymer debris (regime II). This regime was dominated by the 'rolling friction' of debris, which increased μ to 0.72. The increased friction associated with the change from non-rolling 'sliding friction' to 'rolling friction' during the mechanical disintegration of polymer is likely to be due to dissipative effects of 'soft' as opposed to 'hard' materials, and the small size of the particles: the rolling friction force depends on and increases directly with the load, the viscoelastic properties, and inversely with particle size[29,30]. When the load was further increased (up to ~200 mN, regime III), polymer debris was pushed out of the contact area, leaving glass in contact with damaged mica at $\mu = 0.24$, and identical to the sliding of glass on mica without the polymer coating (red curve in Fig. 4). Using epoxy glue as the other surface (which is relatively hydrophobic compared with mica and mimics abrasion with rubber), the polymer coating was peeled off at a minute load ($L < 10$ mN) and manifested only two regimes (regimes II and III, Supplementary Fig. 25). The easier peel-off from the more hydrophobic surface further evidences the importance of hydration layers in resisting erosion by water.

In summary, the use of 'solvent exchange' for engineering polyelectrolyte complexation was shown to offer beneficial properties as a vehicle for wet adhesion and cohesion. Although suppressed in DMSO, electrostatic complexation of dissolved polycations and polyanions is triggered by solvent exchange between water and DMSO, actuating a progression of synergistic changes including coacervation, catechol-mediated interactions, coacervate phase inversion, porosity, solidification and finally wet adhesion. Spatial and temporal progression of the triggered complexation facilitates compelling wet adhesion performances, and exceptional compatibility with diverse material chemistries. For example, by combining the process with bio-inspired catechol chemistry, solvent exchange enabled a rapid and robust wet adhesion on all tested solid surfaces. The wet adhesion energy was dependent on the solvent exchange time, and developed in parallel with the setting time and pore microstructure. The combination of wet adhesion and porous structures makes the universal wet adhesive applicable to fluidics and micro/nano structures (Supplementary Fig. 26), for example, coatings for high-flow regimes with the option of abrasion-dependent removability.

Methods

The catechol-functionalized poly(acrylic acid) (PAAcat) was synthesized and characterized according to our previous method[31] (Supplementary Figs 1–4). Quaternized chitosan with bulk Tf_2N as the counter anion (QCS-Tf_2N) was synthesized by quaternization of chitosan followed by anion exchange (Supplementary Fig. 5).

For wet adhesion processing, QCS-Tf_2N (0.1 g) was dissolved in DMSO (10 ml) at 50 °C under stirring. Then PAAcat (0.15 g) was dissolved into the solution to form a homogeneous blend solution. A trace amount of dye (Rhodamine 6G) was added into the polymer bend solution for better visibility. The polymer blend solution was extruded from a syringe onto substrates submerged in water to sketch any desired pattern on them, and allowed to set in water (20 °C, no applied pressure) for different times. After setting, the adhesive was subjected to water blasting (2–30 bar) to test the wet adhesion. Wet adhesion control experiments were conducted in the same way except the different formulation of the starting polymer solution.

The morphology of the matured adhesive (water setting time 1 h) in the dry state was examined by scanning electron microscopy with energy dispersive spectroscopy (EDS) for element analysis. Morphology of the same adhesive was also measured *in situ* in water by an atomic force microscope (Asylum Research) using an SNL probe ~0.1 N m^{-1} (Bruker) at 22 ± 3 °C in tapping mode. Attenuated total reflectance FTIR spectroscopy of the adhesive coating was performed on a Spectrum Two IR Spectrometer. Fluorescent microscopy for monitoring the solvent exchange was done on an Olympus Fluoview 1000S laser scanning confocal microscope (Supplementary Method 3.2). Adhesion and friction force measurements were performed using Surface Forces Apparatus 2000 (SurForce LLC; see Supplementary Method 3.3 for a detailed explanation of the experimental set-up).

Supplementary Material

Refer to Web version on PubMed Central for supplementary material.

Acknowledgements

The authors gratefully acknowledge financial support from the National Science Foundation (NSF) through the MRSEC Program DMR-1121053 (MRL-UCSB), which also supported the MRL Central Facilities (a member of the NSF-funded Materials Research Facilities Network (www.mrfn.org)). J.H.W. and B.K.A. acknowledge support from the Office of Naval Research N000141310867. J.H.W. and J.N.I. also acknowledge support from the US National Institutes of Health (R01 DE018468). Authors thank R. Mirshafian for help with optical microscope and W. Wei for discussions.

References

1. Faul CFJ, Antonietti M. Ionic self-assembly: facile synthesis of supramolecular materials. Adv. Mater. 2003; 15:673–683.
2. Perry SL, et al. Chirality-selected phase behaviour in ionic polypeptide complexes. Nature Commun. 2015; 6:6052. [PubMed: 25586861]
3. Tang TYD, et al. Fatty acid membrane assembly on coacervate microdroplets as a step towards a hybrid protocell model. Nature Chem. 2014; 6:527–533. [PubMed: 24848239]
4. Sokolova E, et al. Enhanced transcription rates in membrane-free protocells formed by coacervation of cell lysate. Proc. Natl Acad. Sci. USA. 2013; 110:11692–11697. [PubMed: 23818642]
5. Xu LM, et al. Self-assembly of ultralong polyion nanoladders facilitated by ionic recognition and molecular stiffness. J. Am. Chem. Soc. 2014; 136:1942–1947. [PubMed: 24417504]
6. Lee BP, Messersmith PB, Israelachvili JN, Waite JH. Mussel-inspired adhesives and coatings. Annu. Rev. Mater. Res. 2011; 41:99–132. [PubMed: 22058660]
7. Stewart RJ, Ransom TC, Hlady V. Natural underwater adhesives. J. Polym. Sci. B. 2011; 49:757–771.

8. Sedo J, Saiz-Poseu J, Busque F, Ruiz-Molina D. Catechol-based biomimetic functional materials. Adv. Mater. 2013; 25:653–701. [PubMed: 23180685]
9. Zhao H, Sun CJ, Stewart RJ, Waite JH. Cement proteins of the tube-building polychaete Phragmatopoma californica. J. Biol. Chem. 2005; 280:42938–42944. [PubMed: 16227622]
10. Lee H, Lee BP, Messersmith PB. A reversible wet/dry adhesive inspired by mussels and geckos. Nature. 2007; 448:338–342. [PubMed: 17637666]
11. Shao H, Stewart RJ. Biomimetic underwater adhesives with environmentally triggered setting mechanisms. Adv. Mater. 2010; 22:729–733. [PubMed: 20217779]
12. Stewart RJ, Weaver JC, Morse DE, Waite JH. The tube cement of Phragmatopoma californica: a solid foam. J. Exp. Biol. 2004; 207:4727–4734. [PubMed: 15579565]
13. Stevens MJ, Steren RE, Hlady V, Stewart RJ. Multiscale structure of the underwater adhesive of Phragmatopoma californica: a nanostructured latex with a steep microporosity gradient. Langmuir. 2007; 23:5045–5049. [PubMed: 17394366]
14. Tamarin A, Lewis P, Askey J. Structure and formation of byssus attachment plaque in mytilus. J. Morphol. 1976; 149:199–221. [PubMed: 933173]
15. Desmond K, Zacchia NA, Waite JH, Valentine M. Dynamics of mussel plaque detachment. Soft Matter. 2015; 11:6832–6839. [PubMed: 26223522]
16. Bungenberg de Jong, HG. Colloid Science. Kruyt, HR., editor. Vol. II. Elsevier; 1949. p. 431-482.
17. Hwang DS, et al. Viscosity and interfacial properties in a mussel-inspired adhesive coacervate. Soft Matter. 2010; 6:3232–3236. [PubMed: 21544267]
18. Stewart RJ, Wang CS, Shao H. Complex coacervates as a foundation for synthetic underwater adhesives. Adv. Colloid Interface Sci. 2011; 167:85–93. [PubMed: 21081223]
19. Rose S, et al. Nanoparticle solutions as adhesives for gels and biological tissues. Nature. 2014; 505:382–385. [PubMed: 24336207]
20. Ono T, Sugimoto T, Shinkai S, Sada K. Lipophilic polyelectrolyte gels as super-absorbent polymers for nonpolar organic solvents. Nature Mater. 2007; 6:429–433. [PubMed: 17468762]
21. Yuan JY, Mecerreyes D, Antonietti M. Poly(ionic liquid)s: an update. Prog. Polym. Sci. 2013; 38:1009–1036.
22. Poulsen N, et al. Isolation and biochemical characterization of underwater adhesives from diatoms. Biofouling. 2014; 30:513–523. [PubMed: 24689803]
23. Gibson LJ, Ashby MF. The mechanics of 3-dimensional cellular materials. Proc. R. Soc. Lond. A. 1982; 382:43–59.
24. Meyers MA, McKittrick J, Chen PY. Structural biological materials: critical mechanics-materials connections. Science. 2013; 339:773–779. [PubMed: 23413348]
25. Wu DC, et al. Design and preparation of porous polymers. Chem. Rev. 2012; 112:3959–4015. [PubMed: 22594539]
26. Johnson KL, Kendall K, Roberts AD. Surface energy and contact of elastic solids. Proc. R. Soc. Lond. A. 1971; 324:301–313.
27. Raviv U, et al. Lubrication by charged polymers. Nature. 2003; 425:163–165. [PubMed: 12968175]
28. Raviv U, Klein J. Fluidity of bound hydration layers. Science. 2002; 297:1540–1543. [PubMed: 12202826]
29. Ludema KC, Tabor D. The friction and visco-elastic properties of polymeric solids. Wear. 1966; 9:329–348.
30. Israelachvili, JN. Intermolecular and Surface Forces. 3rd edn. Academic; 2011. p. 494
31. Ahn BK, Lee DW, Israelachvili JN, Waite JH. Surface-initiated self-healing of polymers in aqueous media. Nature Mater. 2014; 13:867–872. [PubMed: 25064231]

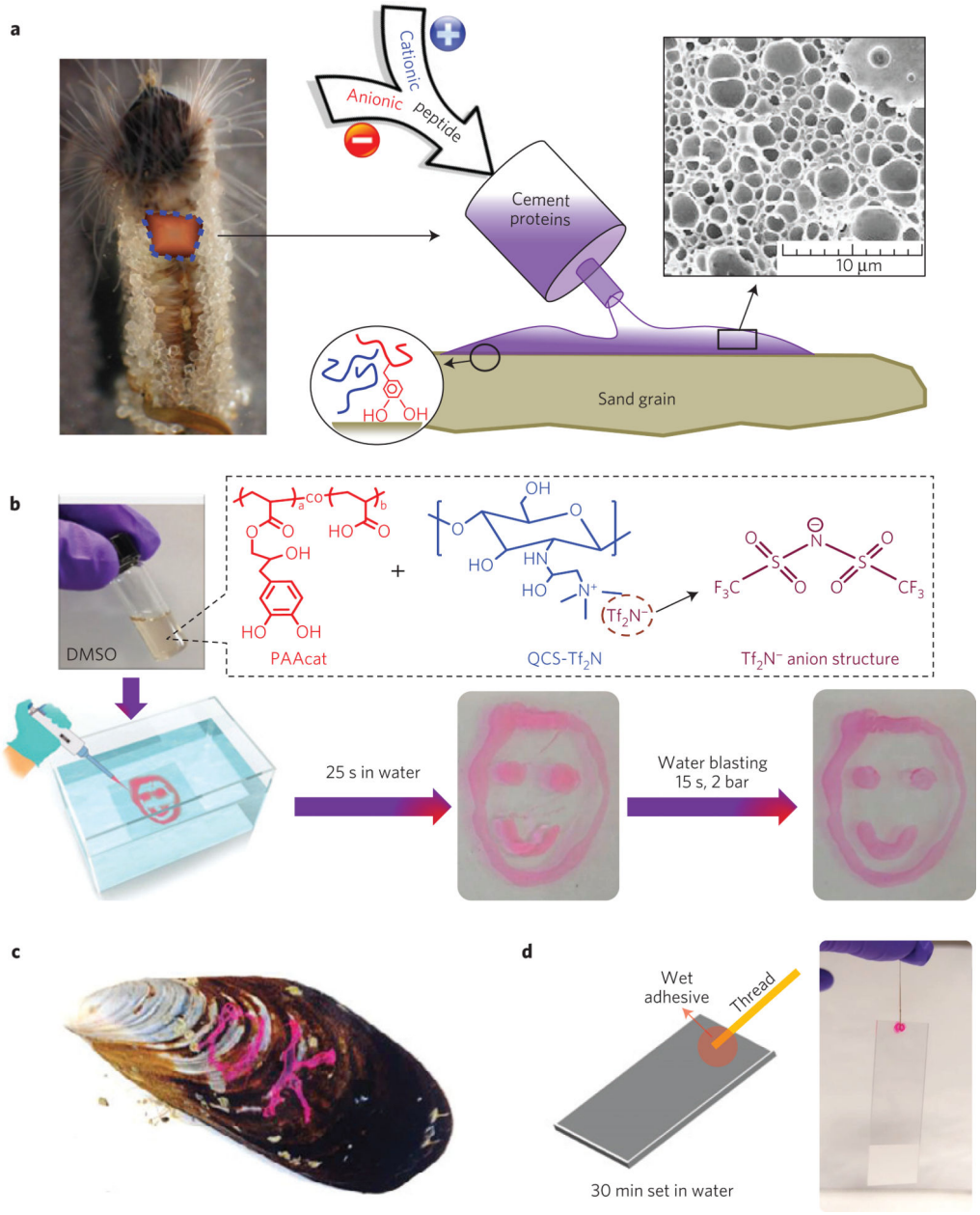

Figure 1. Materials inspiration and underwater adhesion

a, Sandcastle worms (*Phragmatopoma californica*) inhabit tubes made of cemented sand grains. The building organ is highlighted (blue dashed outline) and enlarged to show that the mixing of separately produced polyanionic and polycationic proteins is required for cement adhesion and microarchitecture. **b**, Wet adhesion mediated by solvent exchange: from left to right: QCS-Tf_2N and PAAcat were dissolved in DMSO and the mixture was extruded onto a glass slide immersed in water. After setting 25 s in water (20 °C, no applied pressure), adhesion to substrate withstood water blasting (2 bar, 15 s). Note: sketches are red owing to the addition of trace Rhodamine 6G into the polymer blend solution. **c**, The polymer blend adheres to a mussel shell; more substrates are shown in Supplementary Information (Supplementary Figs 10 and 11). **d**, Polymer blend with embedded cotton thread cast onto a

glass slide in water. After 1 h, adhesion can support the weight of slides in air (60% relative humidity).

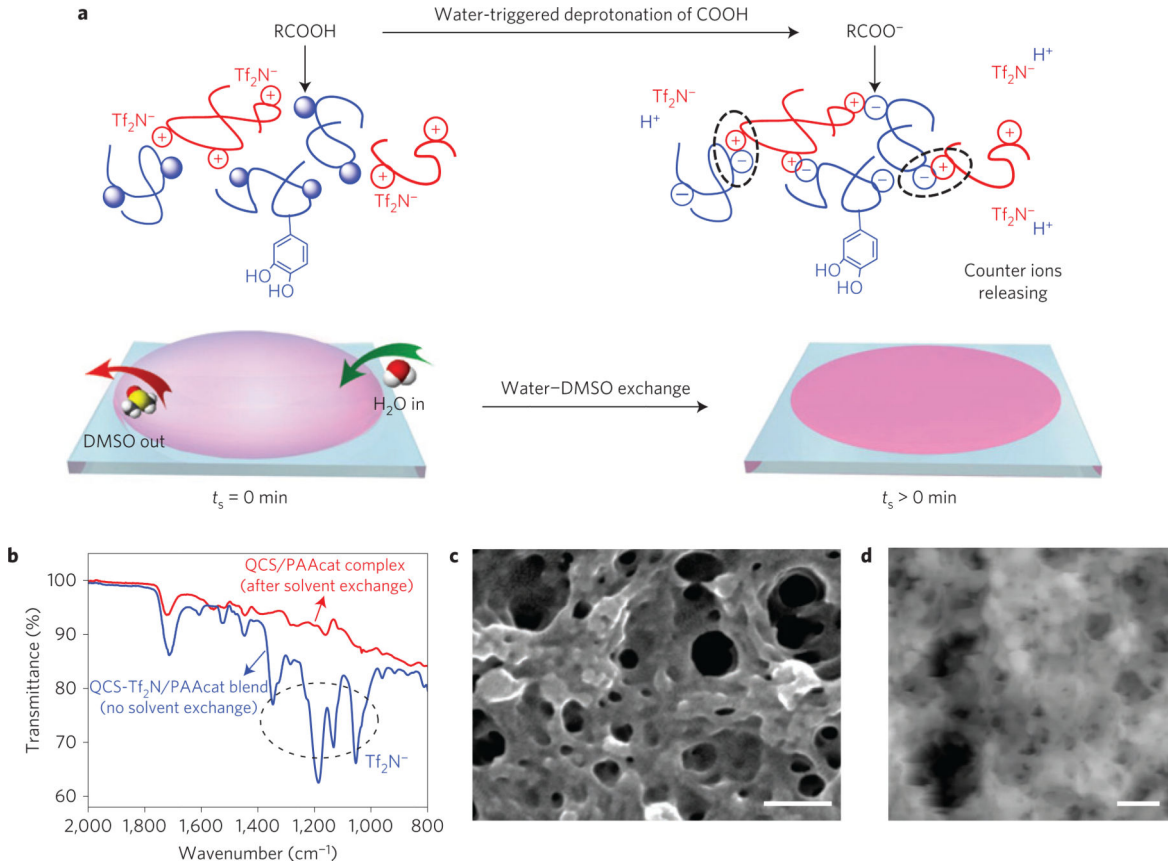

Figure 2. Mechanism and materials characterization

a, An illustration of solvent exchange between water and DMSO and ensuing electrostatic complexation (scheme at top) as a function of setting time in water (t_s). **b**, FTIR of a QCS/PAAcat complex adhesive formed by solvent exchange compared with a physical blend without solvent exchange dried at 80 °C. **c**,**d**, Surface morphology of the QCS/PAAcat adhesive (t_s = 1 h) examined by environmental scanning electron microscopy (**c**), and atomic force microscopy (**d**) *in situ* in water; scale bars in **c**,**d** are 200 nm.

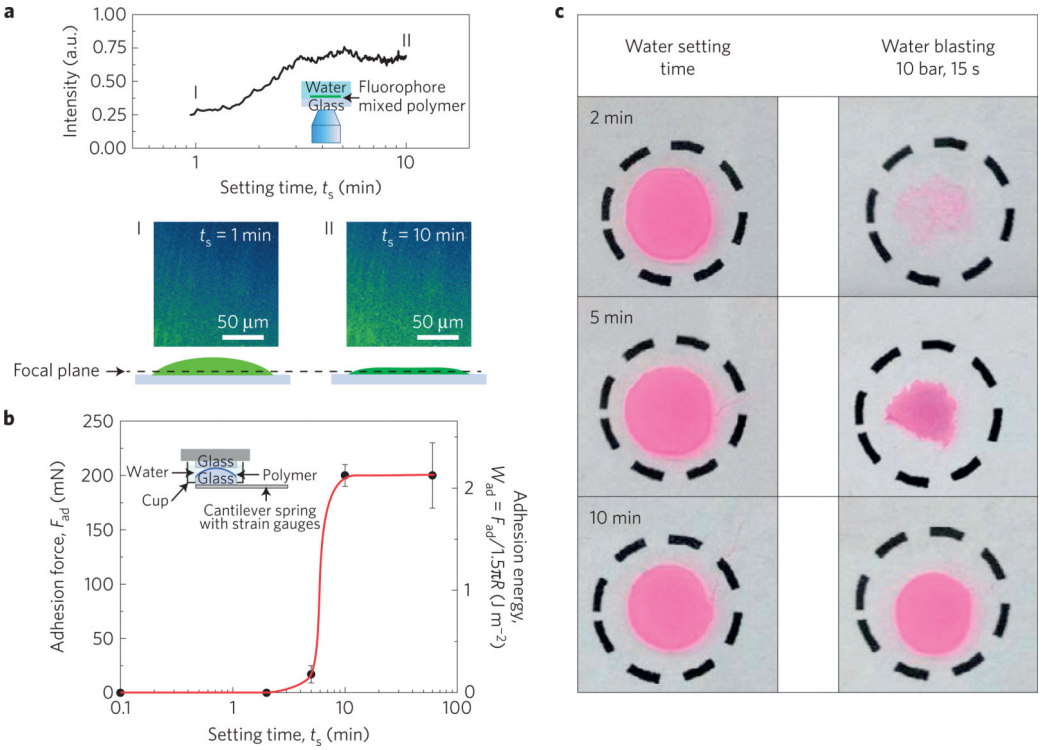

Figure 3. Effect of setting time in water on solvent exchange and adhesion

a, Solvent exchange (water–DMSO) kinetics measured by confocal fluorescent microscopy; note: a fluorescent dye molecule ‘DIL’ (DMSO-soluble and water-insoluble), shown in green, was added to the polymer solution before immersion in water. The intensity of DIL at a specific focal plane was monitored with setting time. Blue colour indicates background (no fluorescence signal). **b**, Effect of setting time on the adhesion force measured by SFA. Error bars are the standard deviation of at least five independent experiments. **c**, Effect of setting time on resistance to water blasting (10 bar, 15 s); the diameter of the dashed black circle is 1 cm.

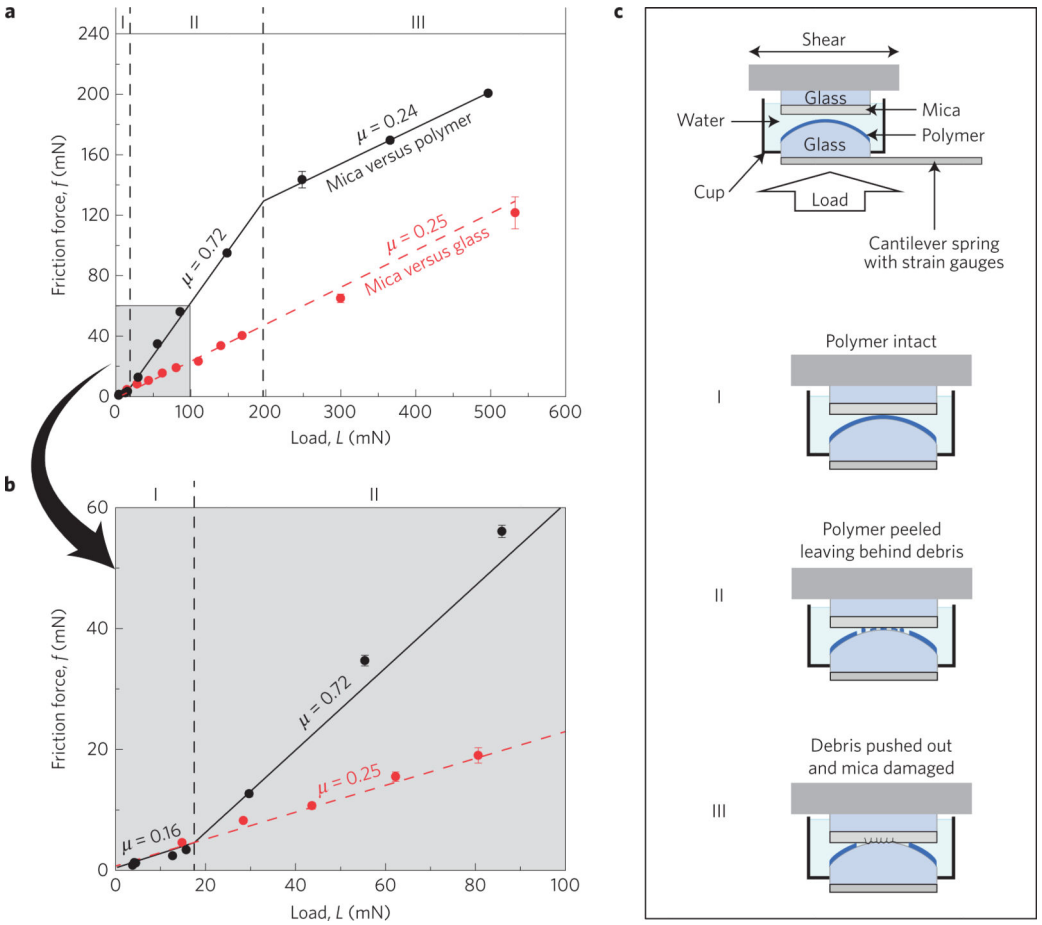

Figure 4. Underwater friction experiments of mica versus adhesive-coated glass performed using an SFA

a, Load versus friction force curves for mica versus polymer (black circles and lines) and mica versus glass (red circles and lines). Error bars are the standard deviation of at least five measured friction forces. **b**, Magnified plot of **a**. **c**, Schematics of friction in the SFA during and following shear.